Climate Oscillations influence on GOM Circulation.

Gabriel Gallegos D.B.[1] and Alejandro J Souza[1]

[1]Departamento de Recursos del Mar, Centro de Investigación y de Estudios Avanzados del Instituto Politécnico Nacional, Unidad Mérida, Km 6 Carretera Antigua a Progreso, 97310, Cordemex, Mérida, Yucatán, México.

Correspondence: Alejandro J Souza (alejandro.souza@cinvestav.mx)

Abstract. Atmosphere-ocean interactions are understood to significantly modulate climate variability and ocean circulation patterns. In this study, the influence of climate oscillations, particularly the North Atlantic Oscillation (NAO) and the El Niño-Southern Oscillation (ENSO), on the circulation dynamics of the Gulf of Mexico (GoM) is investigated. Empirical Orthogonal Function (EOF) analysis was used to identify the principal modes of variability in the GoM circulation, and cross-spectral analysis was conducted to examine the coherence between the GoM circulation, NAO, and ENSO indices. The results reveal that Gulf of Mexico circulation patterns share significant frequencies with both NAO and ENSO. These shared frequencies suggest synchronization phenomena between NAO, ENSO, and the Atlantic Meridional Overturning Circulation (AMOC), indicating a strong influence of these climate oscillations on the GoM's circulation. Key frequencies observed include a near 7-year period aligning with ENSO's natural variability and semiannual periods linked to NAO and the Madden-Julian Oscillation (MJO). These climate oscillations are found to modulate heat transfer intensity in the GoM, influencing large-scale ocean-atmosphere interactions. The findings highlight the critical role of NAO-ENSO teleconnections in shaping GoM circulation variability and their broader implications for global oceanic heat transport mechanisms.

1 Introduction

The upper dynamics ($z \geq 1000m$) of the Gulf of Mexico (GoM) are governed by the Loop Current (LC) (Zavala-Hidalgo et al., 2014). Its natural forcing is the Yucatan Current (YC) (Oey, 2004), through which $23-27Sv$ are transported across the Yucatan Channel (Oey Jr. et al., 2005), with transport variability ranging from $14-36Sv$ in this passage (Sheinbaum et al., 2002). Yucatan current variability has been associated with mesoscale eddies propagating from the Cayman Basin through the Yucatan Channel (Cetina et al., 2006). There is evidence that vorticity coherent structures could improve the understanding of LC variability (Androulidakis et al., 2021).

Although the understanding of LC dynamics remains unclear, several works describe LC behavior through numerical, telemetric, and *in situ* observations (Oey Jr. et al., 2005; DiMarco et al., 2005; Candela et al., 2019; Hall and Leben, 2016). LC sheds energetic anticyclonic eddies with a mean period of eleven months ($f_{LCEddie} \sim 1.09yr^{-1}$), with semiannual and nine-month shedding periods also observed (Sturges and Leben, 2000; Leben, 2005). These eddies import Caribbean Sea Water (CSW) to the northeastern region of the Gulf of Mexico. The vertical structure of this recirculation can reach depths of 600m, characterized by relatively warmer and saltier water than its surroundings. This temperature and salinity gradient decreases as the structure moves westward (Brokaw et al., 2020). Loop Current eddies (LCe) eventually interact with the western boundary of the Gulf of Mexico, with these interactions potentially having profound implications for shelf transport (Guerrero et al., 2020). The warm (anticyclonic) and cold (cyclonic) eddies associated with its circulation behavior have deep implications for connectivity between the Caribbean Sea and the Gulf of Mexico, including effects on primary productivity (Kitchens et al., 2017; Santana-Cisneros et al., 2021) and the Loop Current itself (Damien et al., 2021; Timm et al., 2020).

In addition to LCe, shelf transport in the Gulf of Mexico ($z \sim 200m$) is influenced by wind-generated forcing. On the western border of the Gulf of Mexico shelf, there is a significant correlation between shelf circulation and atmospheric variability (Zavala-Hidalgo et al., 2014). Upwelling events have been observed on the eastern border of the Yucatan shelf ($\sim 200km$ wide) (Merino, 1997; Mariño-Tapia et al., 2014), typically associated with variability in YC strength and position. High-frequency winds contribute approximately $\sim 17\%$ to the upwelled water (Jouanno et al., 2018). Once the upwelled water reaches the Yucatan shelf, wind and shelf circulation propagate subsurface water westward (Reyes-Mendoza et al., 2016; Ruiz-Castillo et al., 2016; Damien et al., 2021). Significant upwelling signatures have also been observed on the western side of the Yucatan shelf and along the western and southern coasts of the Gulf of Mexico (Zavala-Hidalgo et al., 2006).

Evidence suggests that the intensity of the Loop Current has been weakening since the 21st century (Liu et al., 2012). Recent research indicates that this weakening has been occurring since the mid-Pleistocene transition (Huebscher and Nuernberg, 2023). The Loop Current is an integral part of the Atlantic Meridional Overturning Circulation (AMOC) (Bower et al., 2019), a global circulation system whose variability is intricately linked with atmospheric interactions. Intensification or weakening of the AMOC impacts climate variability (Buckley and Marshall, 2016), with positive and negative atmospheric feedback (Huang et al., 2014). Atmosphere-Ocean interaction exchanges a large amount of energy, potentially enhancing or weakening AMOC intensity and thereby heat transport from tropical to northern latitudes (Jackson et al., 2022; Trenberth and Fasullo, 2017). Variability in heat transport can induce regional climate changes and interact with climate oscillations such as the North Atlantic Oscillation (NAO), which governs main winter variability in southern Europe and the northwestern Atlantic (Castro-Díez et al., 2002). Recent research indicates a link between ENSO and AMOC variability at interannual frequencies (Smith and Polvani, 2021), with this interaction potentially contributing significantly to weakening or enhancing the El Niño Southern Oscillation (ENSO), with up to a $\sim 95\%$ reduction in extreme cases (Orihuela-Pinto et al., 2022). Possible interactions between NAO and ENSO have been reported due to teleconnections and the weakening or strengthening of the upper wind jet stream, NAO-driven by the seasonal ENSO-driven variability of the Pacific Jet Stream (Mezzina et al., 2020).

This work focuses on the variability of Gulf of Mexico circulation, primarily driven by the Loop Current linked to AMOC (Pietrafesa et al., 2022), and climate oscillations, particularly ENSO and NAO, which have been linked to AMOC intensity variability. This will be achieved through a combination of EOF and frequency analysis using numerical outputs (ORCA-NEMO) for oceanic currents, and inclusion of ENSO and NAO Index Oscillations in the analysis.

2 Methods

1. Dataset Description

The dataset for this study is based on the ORCA12 circulation model, a high-resolution configuration within the Nucleus for European Modelling of the Ocean (NEMO) framework. NEMO is a flexible and modular ocean modeling platform that simulates ocean circulation, sea-ice dynamics, and biogeochemical cycles. It includes key components such as OPA (Ocean Parallelise), which handles large-scale ocean circulation, and SI3 (Sea Ice model, 3rd generation), which simulates sea-ice dynamics and thermodynamics. This versatility makes NEMO suitable for both global and regional studies.

The ORCA12 configuration uses a tripolar ORCA grid, avoiding singularities at the North Pole by shifting the poles over land in Canada, Russia, and Antarctica, ensuring accurate simulations in polar regions. ORCA12 operates at a 1/12° horizontal resolution, ideal for capturing fine-scale oceanic features, such as eddies and currents, crucial for understanding ocean dynamics in the Gulf of Mexico (GoM). The dataset spans 58 years, from 1958 to 2015, and is forced by the Drakkar Forcing Set (DFS4.1), incorporating realistic atmospheric conditions (Marzocchi et al., 2015). The ORCA vertical configuration is set up in sigma coordinates and then interpolated in a z-coordinate system, where vertical resolution decreases with depth. In the upper $200m$, the resolution varies from $\sim 1m$ at the first levels to $\sim 20m$ at the near $200m$ depth. This stricture ensures that surface circulation and climate-driven variability, are well solved. As the depth is increased the Δz is increased reaching $\sim 200m$ at the deepest values.

Additionally, large-scale climate oscillation data, including the North Atlantic Oscillation (NAO) and El Niño-Southern Oscillation (ENSO) using the Oceanic Niño Index (ONI), are integrated to explore their impacts on GoM circulation. These indices are significant climate drivers influencing global oceanic and atmospheric conditions, affecting the Atlantic Meridional Overturning Circulation (AMOC) and ocean circulation patterns. This study uses these indexes to examine their influence on the GoM's long-term variability (Blaker et al., 2015; Duchez et al., Sep 2014).

2. EOF - GoM Circulation

Empirical Orthogonal Function (EOF) analysis was performed on the ORCA12 model data to identify the dominant patterns of variability in the Gulf of Mexico (GoM). In this analysis the horizontal surface currents were taken as the average of the first 200 m of the water column meters, to apply the EOF analysis, the horizontal vector current was treated as a complex number: $u + iv$. This technique allows the horizontal velocity to be decomposed into spatial patterns on the surface circulation, referred to as EOF modes, and their corresponding temporal variations, known as Principal Components (PCs). The first four modes of variability, which capture the largest portion of variability ($\sim 50\%$) in the GoM circulation, were extracted.

The temporal evolution of these spatial patterns, represented by the PCs, was analyzed to reflect how the dominant patterns change over time. A significance test was conducted to ensure the robustness of the results, comparing the eigenvalues obtained from the EOF analysis with those derived from a white noise dataset. This comparison was used to confirm that the identified modes represent meaningful patterns, rather than random fluctuations (North et al., 1982).

3. **Cross-Spectral Analysis**

To explore the relationship between GoM circulation variability and large-scale climate oscillations, a cross-spectral analysis was performed between the Principal Components (PCs) of the EOF modes and major climate indices, including the NAO and ENSO (ONI). This analysis examined coherence and phase relationships in the frequency domain, identifying connections between the temporal variability in GoM circulation and large-scale oscillations.

The Atlantic Meridional Overturning Circulation (AMOC) is known to be influenced by the NAO through mechanisms related to deep water formation in the North Atlantic. Positive phases of the NAO enhance the formation of deep water, strengthening the AMOC, while negative phases have the opposite effect (Marzocchi et al., 2015; Blaker et al., 2015; Duchez et al., Sep 2014). Similarly, the ENSO impacts the AMOC through variations in heat transport that influence atmospheric circulation patterns and oceanic conditions in the tropical Pacific, which in turn affect the North Atlantic (Marzocchi et al., 2015; Blaker et al., 2015). These climate oscillations are significant drivers of variability in the GoM circulation, making the cross-spectral analysis a valuable tool for understanding their influence.

3 Results and Discussion

The EOF analysis from GoM circulation ($200m$ mean) shown in Figure1. The principal components of the latest data were analysed with ENSO and NAO indexes through cross spectra, the latest results are shown in Figure 2.

3.1 EOF

The EOF analysis of the Gulf of Mexico (GoM) circulation reveals significant insights into the spatial and temporal variability of the region's dynamics (Figure 1). The spatial description of the deep GoM EOF modes hihghlight different states of Loop Current (LC) and the westward moving of LCE's along the GoM deep waters (Sturges and Leben, 2000; Leben, 2005; Zavala-Hidalgo et al., 2003; Sturges and Kenyon, 2008). The highest kinetic energy variability for all EOF modes is concentrated in the Yucatan Channel and the Florida Strait, while areas outside the GoM outer shelf (200m), represented by the dashed marine blue line (Figure 1) show less variability. Circulation variability on the GoM shelf decreases by at least one order of magnitude at the northern shelf and by two orders of magnitude on the Yucatan shelf (western side).

Each EOF mode describes the circulation variability contribution with linear independence from the other modes. The first spatial mode centers the most intense signal in the Yucatan Channel and the Florida Strait, representing the mean position of the Loop Current. It also indicates a recirculation pattern with a lesser order of magnitude ($\sim 10^{-1}$). As the mode number increases (indicating decreased described variability), the recirculation patterns in the inner GoM become more significant. These patterns can be interpreted as an energy transfer from the LC to the inner GoM through LCEs (Yang et al., 2020; Candela et al., 2002). The total described variance for GoM circulation in four modes is $\%51.83$. The fifth and hihger EOF modes were not significative compared to the error white noise values.

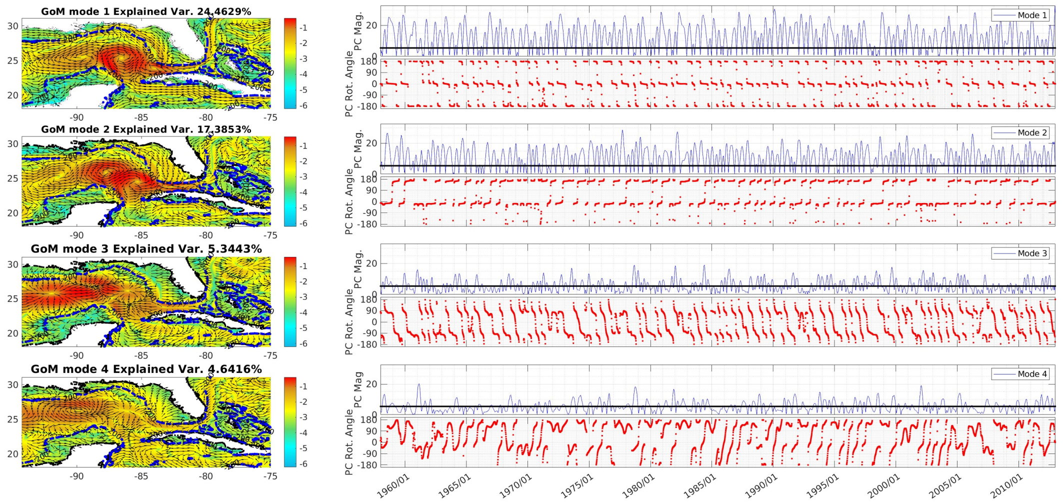

Figure 1. GoM Circulation EOF. Left panel en each figure shows the spatial variability, color bar shows variability logarithmic amplitude. Right panel shows temporal variability expressed as magnitude (blue) and rotation angle (red dots) The rotation follows a geometric convention, where positive angles indicate counterclockwise rotation from the east. The solid blue horizontal line on each PC's that represents the white noise magnitude for the equivalent ORCA data matrix. The PC oscillations exhibit increased amplitude as a consequence of scaling EOF's to unit variance during the Kaiser Normalization process, ensuring total variance conservation.

EOF Mode 2 captures the Loop Current eddy-shedding process, where large warm-core anticyclonic eddies (Loop Current Eddies, LCEs) detach and drift westward into the central Gulf of Mexico (GoM).

EOF Mode 3 represents the westward propagation of Loop Current Eddies (LCEs) and their interaction with the deeper ocean circulation. Detached LCEs gradually lose energy as they interact with bottom topography.

EOF Mode 4, unlike the first three modes, which primarily describe LC structural changes, reflects variability induced by external forcing mechanisms, such as wind stress fluctuations. In this mode, LCEs appear less structured, and variability over

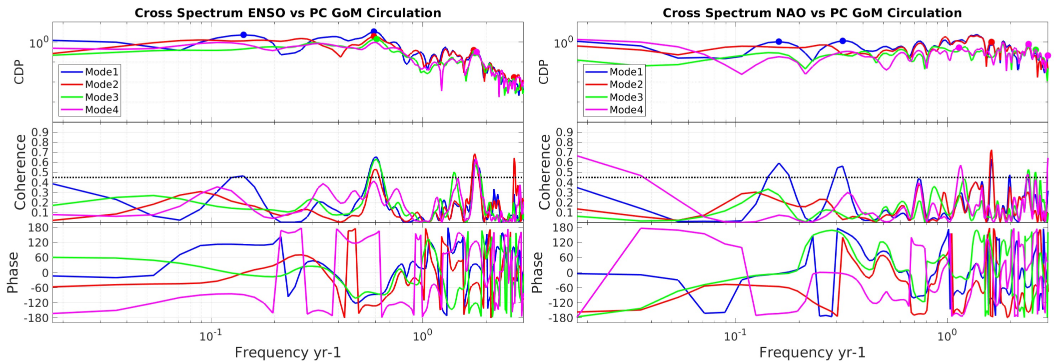

Figure 2. Cross spectra for GoM Circulation. Left panels show ENSO-GoM correlation. Right panel NAO-GoM circulation results are presented. Top panels show Cross Spectra Power Density (CPD). Center panels present coherence values. Bottom panel show the phase between GoM velocity field and climate oscillations.

the continental shelf becomes more significant.

3.2 Cross spectra analysis

The cross-spectral analysis identifies key frequencies associated with the GoM circulation patterns and their coherence with ENSO and NAO. This analysis provides insights into the coherence and phase relationships between these climate indices and the GoM circulation for each decomposed modes.

Several researches have pointed out the atmosphere-ocean coupled system and how does the circulation patterns can transfer thermal energy from distant places on the earth (Mezzina et al., 2020; Feng et al., 2017; Jaramillo et al., 2021), through different physical mechanisms. These energy fluctuations have the potential to enhance or diminish climatic oscillations . The ENSO-GoM circulation cross spectra will be presented first followed by the AMOC-GoM analysis. Figure2 shows the GoM circulation shared frequencies, with the ENSO (left panel) and the NAO (right panel) indices. The significant shared frequencies (coherence > 0.45) are highlighted by colored dots, each color is consistent with the EOF-Mode, the coherent shared frequencies will be described and discussed below starting with the ENSO-GoM and then tne NAO-GoM interactions.

1. ENSO - GoM shared frequencies.

- First EOF mode have significant shared frequency at $f = 0.1425y^{-1} \implies T = 7.01y$. This frequency aligns with ENSO in its natural frequency variability $T_{ENSO} \sim 5 - 7y$ (Bruun et al., 2017). In GoM circulation this frequency can be associated to the LC length variability which its natural frequency (Leben, 2005) $f_{LC} = 0.1791y^{-1}$.
- First, second and third GoM PC modes share energy with ENSO at $f = 0.6059y^{-1}$. This frequency concordance could be modulated by typical ENSO duration (12-18 months) (McPhaden, 2002). In the GoM circulation natural frequencies the shared oscillation fits to the 18 months eddies shedding frequency , which is also related to the $T \sim 17$ months of length LC variability (Leben, 2005)

- Near semiannual frequencies $f = 1.771y{-}1$ also are shared by all EOF-GoM circulation modes and ENSO index. The source from the high frequency oscillation could be the interaction between the Madden Jullien Oscillation (MJO), the results of this interaction could lead significant variability in global weather patterns at seasonal and higher frequencies (Li et al., 2021; Jiang et al., 2020). In particular can reduce or strength the seasonal transitions.

Most physical arguments connecting ENSO to AMOC modulation points towards heat and salinity distribution through distinct mechanisms, such as enhancing or weakening storms over the Atlantic and GoM (McPhaden, 2002), particularly during high meltwater flux periods (Orihuela-Pinto et al., 2022; Liu et al., 2014). The ocean-atmosphere feedback interactions have distinct timescale responses due the differences of density, specific heat and intrinsic properties (McPhaden, 2002), causing a natural lag and shift frecuencies and phases of oscillation for each coupled system.

The natural lag and frequency shifts of oscillations for each coupled system were analyzed, identifying significant values presented in the following table. The phases are expressed in time lag (years), providing insight into the temporal relationships between the signals. The ENSO index was selected as the leading reference signal for this analysis (Table 1).

Mode	Frequency (cpy)	CPD	Coherence	Phase (°)	Phase (radians)	Time Lag (years)
1	0.5881	3.2987	0.6512	-87.5216	-1.5275	-0.4134
1	1.7466	0.2889	0.5886	31.4135	0.5483	0.0500
2	0.5881	1.8183	0.5059	-142.664	-2.4900	-0.6738
2	1.7466	0.3040	0.6614	-54.3485	-0.9486	-0.0864
2	2.7090	0.0096	0.6761	-32.2751	-0.5633	-0.0331

Table 1. ENSO-GoM Circulation significant shared frequencies.

2. NAO -GoM shared frequencies

- First (blue) and third (green) NAO-GoM circulation mode shows shared frequencies at $f = 0.1604y^{-1}$, and $f = 0.1428y^{-1}$ respectively. These frequencies are near the NAO natural oscillation frequency $f_{NAO} \sim 0.17y^{-1}$ (Massei et al., 2007; Hurrell et al., 2003).For the GoM circulation first mode correlates the LC length natural period $T_{LC} = 67$months (Leben, 2005)

- First mode GoM circulation also shares energy with NAO at $f = 0.3208y^{-1}$. NAO also has a natural oscillation frequency at $f_{NAO} \sim 0.3y^{-1}$ (Massei et al., 2007; Hurrell et al., 2003). At the GoM current variability it has been found that LC could be a nonlinear oscillator which has $3-5y$ period with highly influenced by the NAO (Lugo-Fernández, 2007).

- Fourth GoM mode (pink) has a near-yearly frequency as the NAO natural oscillation (Pozo-Vázquez et al., 2000). The spectral analysis results also show seasonal shared frequencies potentially related to the MJO modulation (Lin et al., 2009). In GoM circulation description the $f \sim 1y^{-1}$ frequency corresponds to an 11-month ring shedding period and a coherent LC length, as well as semiannual periods (Leben, 2005).

- First and Second GoM modes share a $f \sim 1.6y{-}1$ frequency with NAO alignin with the $f \sim 1.7y^{-1}$ found in ENSO-GoM analysis. This suggest that summer-winter transition could be a strong modulation signal. The MJO could be a potential enhancing or weakening effect on this processes (Wu et al., 2006)

The NAO-AMOC interactions have a geographically direct relationship. Positive NAO phases increase ocean-atmosphere heat flux and deep water formation, strengthening the AMOC (Hurrell et al., 2003; Delworth and Zeng, 2016). Negative NAO phases is expected to weaken the AMOC intensity. NAO's influence on GoM circulation more pronounced in lower frequencies for the most significant variability EOF first mode (42% described variability). However higher modes (less explained variability) show significant shared frequencies at seasonal periods. Shelf sea variability has strong seasonal frequency input, with wind dynamics winter (nortes) and summer (tropical storms). Both escenarios can be modulated by ENSO trough atmospheric teleconnections (Mezzina et al., 2020; Feng et al., 2017).

As the understanding on heat fluxes and connectivity of distinct climate oscillations improves, the global interconnection among them has become each time more evident (Liu et al., 2023; Misra, 2020). Ocean-atmosphere feedback (Watanabe and Kimoto, 2000) plays a fundamental role in spatiotemporal heat dynamics. Changes in a single element *e.g.* the consequences on ocean circulation due the increased heat capacity in the atmosphere due to rising CO_2 levels, can drive deep changes in thermohaline circulation is a phenomenon studied since the last century (Stocker and Schmittner, 1997).

NAO and ENSO are oscillating systems (Bruun et al., 2017; Hurrell et al., 2003) with characteristic frequencies that could be described as a spectral signature, similar to LC description (Lugo-Fernández, 2007). These three elements are interconnected and modulated in distinct levels by each other, forming a coupled oscillation network where each element has feedback with each other.

A similar analysis was conducted for the NAO-GoM coupled system, following the same methodology as in the ENSO-GoM case. The significant values are presented in the following table, with phases expressed in time lag (years) and the NAO index selected as the leading reference signal (Table 2).

Mode	Frequency (cpy)	CPD	Coherence	Phase (°)	Phase (radians)	Time Lag (years)
1	0.1604	1.0607	0.6243	-4.767	-0.0832	-0.0826
1	0.3208	1.1484	0.5491	166.0534	2.8982	1.4378
1	1.6218	0.7705	0.6478	-103.1568	-1.8004	-0.1767
2	1.6040	0.8303	0.6941	178.2975	3.1119	0.3088
3	2.4238	0.3828	0.5251	24.4508	0.4267	0.0280
3	2.6199	0.2053	0.4897	161.9329	2.8263	0.1717
4	0.1604	0.5029	0.4823	-130.9301	-2.2852	-2.2674
4	0.3208	0.7625	0.5942	30.4282	0.5311	0.2635
4	0.7307	0.5408	0.5655	160.4626	2.8006	0.6100
4	1.1941	0.5882	0.4824	-75.5393	-1.3184	-0.1757

Table 2. NAO-GoM Circulation Time Lags

4 Conclusions

GoM circulation EOF modes, describes the system variability as LCE's are propagated to the west of the GoM basin. These eddies are subscribed outside of the outer shelf ($h > 200m$). Shelf variability has at least an order of magnitude less than the LCE's governed dynamics zone (Figure 1,spatial variability EOF maps).

Frequency analysis has show a correlated variability for interannual frequencies with ENSO and NAO. These shared frequencies are associated with LC length variability and LCE's shedding frequency (Leben, 2005) in the GoM circulation patterns on one hand and natural oscillation frequencies for the climate oscillations on the other.

Seasonal shared frequencies are more related to ENSO-NAO teleconections and its influences on climate variability, such as winter (Nortes) and summer (Tropical cyclonic activity) atmosphere energy inputs. For both NAO and ENSO cross spectra results, higher shared frequencies for GoM circulation are dominated by higher EOF modes, hence lower variability explained, this could be associated to the variability on the GoM shelf seas, that have a better response to atmospheric forcing (seasonal frequencies), also the MJO interactions with NAO and ENSO could play an important role in the higher coherent frequencies.

Coherent energy shared between climate oscillation (NAO, ENSO) and GoM circulation are mainly concentrated at $5-7y$, $1.6y$, and nearly semianual periods, $1.6667y$ for ENSO-GoM circulation. Shared energy for NAO-GoM circulation have coherent shared frequencies at $6.6y$, $3.1y$, and ~ 11 months periods.

Future work. These coherent oscillation systems can be conceived as a complex oscillator network driven by spatiotemporal patterns of heat exchange. Teleconnections act as pathways for distributing heat gradients across seemingly distant regions, creating atmospheric "road maps" of heat transport, primarily influenced by Rossby waves. Traditionally, climatic oscillations such as the NAO, ENSO, and QBO have been understood individually. However, these spatiotemporal heat gradient patterns can instead be represented as interconnected elements of a broader system, analogous to pendulums linked within a complex oscillator network. This network is interconnected through two major "highways" of heat transport: (1)the atmospheric pathway dominated by Rossby waves, and (2) the oceanic pathway governed by the thermohaline circulation that redistribute heat across distant points on Earth. Framing climate variability in terms of this complex oscillator system provides a unified perspective, capturing the intricate interplay of independent oscillations and their role in shaping global climate dynamics.

Author contributions. **Gabriel Gallegos D.B.** Conceptualization, formal analysis, methodology, project administration, visualization, writing - original draft preparation. **Alejandro J. Souza** Conceptualización, methodology, supervision, writing - review and editing, project management.

Competing interests. The authors declare that they have no conflict of interest.

Acknowledgements. Contains data supplied by the UK Natural Environment Research Council. licensed under the Open Government License v1.0 https://gws-access.jasmin.ac.uk/public/nemo/
Contains data supplied by the Climate Prediction Center, NOAA https://www.cpc.ncep.noaa.gov/products/precip/CWlink/MJO/climwx.shtml
Gabriel Gallegos wants to thank CONACYT for the postdoctoral fellowship provided. Part of the analysis was funded by CONAHCYT grant 319258

References

Androulidakis, Y., Kourafalou, V., Olascoaga, M. J., Beron-Vera, F. J., Le Hénaff, M., Kang, H., and Ntaganou, N.: Impact of Caribbean Anticyclones on Loop Current variability, Ocean Dynamics, 71, 935–956, https://doi.org/10.1007/s10236-021-01474-9, 2021.

Blaker, A. T., Hirschi, J. J.-M., McCarthy, G., Sinha, B., Taws, S., Marsh, R., Coward, A., and de Cuevas, B.: Historical analogues of the recent extreme minima observed in the Atlantic meridional overturning circulation at 26°N, Climate Dynamics, 44, 457–473, https://doi.org/10.1007/s00382-014-2274-6, 2015.

Bower, A., Lozier, S., Biastoch, A., Drouin, K., Foukal, N., Furey, H., Lankhorst, M., Rühs, S., and Zou, S.: Lagrangian Views of the Pathways of the Atlantic Meridional Overturning Circulation, Journal of Geophysical Research: Oceans, 124, 5313–5335, https://doi.org/https://doi.org/10.1029/2019JC015014, 2019.

Brokaw, R. J., Subrahmanyam, B., Trott, C. B., and Chaigneau, A.: Eddy Surface Characteristics and Vertical Structure in the Gulf of Mexico from Satellite Observations and Model Simulations, Journal of Geophysical Research: Oceans, 125, e2019JC015 538, https://doi.org/https://doi.org/10.1029/2019JC015538, e2019JC015538 2019JC015538, 2020.

Bruun, J. T., Allen, J. I., and Smyth, T. J.: Heartbeat of the Southern Oscillation explains ENSO climatic resonances, Journal of Geophysical Research: Oceans, 122, 6746–6772, https://doi.org/https://doi.org/10.1002/2017JC012892, 2017.

Buckley, M. W. and Marshall, J.: Observations, inferences, and mechanisms of the Atlantic Meridional Overturning Circulation: A review, Reviews of Geophysics, 54, 5–63, https://doi.org/https://doi.org/10.1002/2015RG000493, 2016.

Candela, J., Sheinbaum, J., Ochoa, J., Badan, A., and Leben, R.: The potential vorticity flux through the Yucatan Channel and the Loop Current in the Gulf of Mexico, Geophysical Research Letters, 29, 16–1–16–4, https://doi.org/https://doi.org/10.1029/2002GL015587, 2002.

Candela, J., Ochoa, J., Sheinbaum, J., López, M., Pérez-Brunius, P., Tenreiro, M., Pallàs-Sanz, E., Athié, G., and Arriaza-Oliveros, L.: The Flow through the Gulf of Mexico, Journal of Physical Oceanography, 49, 1381 – 1401, https://doi.org/https://doi.org/10.1175/JPO-D-18-0189.1, 2019.

Castro-Díez, Y., Pozo-Vázquez, D., Rodrigo, F. S., and Esteban-Parra, M. J.: NAO and winter temperature variability in southern Europe, Geophysical Research Letters, 29, 1–1–1–4, https://doi.org/https://doi.org/10.1029/2001GL014042, 2002.

Cetina, P., Candela, J., Sheinbaum, J., Ochoa, J., and Badan, A.: Circulation along the Mexican Caribbean coast, Journal of Geophysical Research: Oceans, 111, https://doi.org/https://doi.org/10.1029/2005JC003056, 2006.

Damien, P., Sheinbaum, J., Pasqueron de Fommervault, O., Jouanno, J., Linacre, L., and Duteil, O.: Do Loop Current eddies stimulate productivity in the Gulf of Mexico?, Biogeosciences, 18, 4281–4303, https://doi.org/10.5194/bg-18-4281-2021, 2021.

Delworth, T. L. and Zeng, F.: The Impact of the North Atlantic Oscillation on Climate through Its Influence on the Atlantic Meridional Overturning Circulation, Journal of Climate, 29, 941 – 962, https://doi.org/10.1175/JCLI-D-15-0396.1, 2016.

DiMarco, S. F., Nowlin Jr., W. D., and Reid, R. O.: A Statistical Description of the Velocity Fields from Upper Ocean Drifters in the Gulf of Mexico, pp. 101–110, American Geophysical Union (AGU), ISBN 9781118666166, https://doi.org/https://doi.org/10.1029/161GM08, 2005.

Duchez, A., Hirschi, J. J.-M., Cunningham, S. A., Blaker, A. T., Bryden, H. L., de Cuevas, B., Atkinson, C. P., McCarthy, G. D., Frajka-Williams, E., Rayner, D., Smeed, D., and Mizielinski, M. S.: A New Index for the Atlantic Meridional Overturning Circulation at 26°N, Journal of Climate, 27, 6439–6455, https://doi.org/DOI:10.1175/JCLI-D-13-00052.1, Sep 2014.

Feng, J., Chen, W., and Li, Y.: Asymmetry of the winter extra-tropical teleconnections in the Northern Hemisphere associated with two types of ENSO, Climate Dynamics, 48, 2135–2151, https://doi.org/10.1007/s00382-016-3196-2, 2017.

Guerrero, L., Sheinbaum, J., Mariño-Tapia, I., González-Rejón, J. J., and Pérez-Brunius, P.: Influence of mesoscale eddies on cross-shelf exchange in the western Gulf of Mexico, Continental Shelf Research, 209, 104 243, https://doi.org/https://doi.org/10.1016/j.csr.2020.104243, 2020.

Hall, C. A. and Leben, R. R.: Observational evidence of seasonality in the timing of loop current eddy separation, Dynamics of Atmospheres and Oceans, 76, 240–267, https://doi.org/https://doi.org/10.1016/j.dynatmoce.2016.06.002, the Loop Current Dynamics Experiment, 2016.

Huang, B., Zhu, J., and Yang, H.: Mechanisms of Atlantic Meridional Overturning Circulation (AMOC) variability in a coupled ocean-atmosphere GCM, Advances in Atmospheric Sciences, 31, 241–251, https://doi.org/10.1007/s00376-013-3021-3, 2014.

Huebscher, C. and Nuernberg, D.: Seismic and geologic data from southern Gulf of Mexico imply a weakening of the Loop Current since the Mid Pleistocene Transition, in: EGU General Assembly, pp. 24–28, Vienna, https://doi.org/10.5194/egusphere-egu23-3859, 2023.

Hurrell, J. W., Kushnir, Y., Ottersen, G., and Visbeck, M.: An overview of the North Atlantic oscillation, Geophysical Monograph-American Geophysical Union, 134, 1–36, 2003.

Jackson, L. C., Biastoch, A., Buckley, M. W., Desbruyères, D. G., Frajka-Williams, E., Moat, B., and Robson, J.: The evolution of the North Atlantic Meridional Overturning Circulation since 1980, Nature Reviews Earth & Environment, 3, 241–254, https://doi.org/10.1038/s43017-022-00263-2, 2022.

Jaramillo, A., Dominguez, C., Raga, G., and Quintanar, A. I.: The Combined QBO and ENSO Influence on Tropical Cyclone Activity over the North Atlantic Ocean, Atmosphere, 12, https://doi.org/10.3390/atmos12121588, 2021.

Jiang, X., Adames, A. F., Kim, D., Maloney, E. D., Lin, H., Kim, H., Zhang, C., DeMott, C. A., and Klingaman, N. P.: Fifty Years of Research on the Madden-Julian Oscillation: Recent Progress, Challenges, and Perspectives, Journal of Geophysical Research: Atmospheres, 125, e2019JD030 911, https://doi.org/https://doi.org/10.1029/2019JD030911, e2019JD030911 2019JD030911, 2020.

Jouanno, J., Pallàs-Sanz, E., and Sheinbaum, J.: Variability and Dynamics of the Yucatan Upwelling: High-Resolution Simulations, Journal of Geophysical Research: Oceans, 123, 1251–1262, https://doi.org/https://doi.org/10.1002/2017JC013535, 2018.

Kitchens, L. L., Paris, C. B., Vaz, A. C., Ditty, J. G., Cornic, M., Cowan, J. H., and Rooker, J. R.: Occurrence of invasive lionfish (Pterois volitans) larvae in the northern Gulf of Mexico: characterization of dispersal pathways and spawning areas, Biological Invasions, 19, 1971–1979, https://doi.org/10.1007/s10530-017-1417-1, 2017.

Leben, R. R.: Altimeter-Derived Loop Current Metrics, pp. 181–201, American Geophysical Union (AGU), ISBN 9781118666166, https://doi.org/https://doi.org/10.1029/161GM15, 2005.

Li, T., Wang, L., and Hu, F.: Recent advances in understanding MJO propagation dynamics, Science Bulletin, 66, 2448–2452, https://doi.org/https://doi.org/10.1016/j.scib.2021.08.005, 2021.

Lin, H., Brunet, G., and Derome, J.: An Observed Connection between the North Atlantic Oscillation and the Madden–Julian Oscillation, Journal of Climate, 22, 364 – 380, https://doi.org/10.1175/2008JCLI2515.1, 2009.

Liu, T., Chen, D., Yang, L., Meng, J., Wang, Z., Ludescher, J., Fan, J., Yang, S., Chen, D., Kurths, J., Chen, X., Havlin, S., and Schellnhuber, H. J.: Teleconnections among tipping elements in the Earth system, Nature Climate Change, 13, 67–74, https://doi.org/10.1038/s41558-022-01558-4, 2023.

Liu, Y., Lee, S.-K., Muhling, B. A., Lamkin, J. T., and Enfield, D. B.: Significant reduction of the Loop Current in the 21st century and its impact on the Gulf of Mexico, Journal of Geophysical Research: Oceans, 117, https://doi.org/https://doi.org/10.1029/2011JC007555, 2012.

Liu, Z., Lu, Z., Wen, X., Otto-Bliesner, B. L., Timmermann, A., and Cobb, K. M.: Evolution and forcing mechanisms of El Niño over the past 21,000 years, Nature, 515, 550–553, https://doi.org/10.1038/nature13963, 2014.

Lugo-Fernández, A.: Is the Loop Current a Chaotic Oscillator?, Journal of Physical Oceanography, 37, 1455 – 1469, https://doi.org/10.1175/JPO3066.1, 2007.

Mariño-Tapia, I., Enríquez, C. E., Reyes-Mendoza, O., and Herrera-Silveira, J.: On the dynamics of upwelling events in the Yucatan Shelf using in situ observations, in: Proc. 17th Physics of Estuaries and Coastal Seas (PECS) Conf., Porto de Galinhas, Pernambruco, Brazil, 19–24 October 2014, 2014.

Marzocchi, A., Hirschi, J. J.-M., Holliday, N. P., Cunningham, S. A., Blaker, A. T., and Coward, A. C.: The North Atlantic subpolar circulation in an eddy-resolving global ocean model, Journal of Marine Systems, 142, 126–143, https://doi.org/https://doi.org/10.1016/j.jmarsys.2014.10.007, 2015.

Massei, N., Durand, A., Deloffre, J., Dupont, J. P., Valdes, D., and Laignel, B.: Investigating possible links between the North Atlantic Oscillation and rainfall variability in northwestern France over the past 35 years, Journal of Geophysical Research: Atmospheres, 112, https://doi.org/https://doi.org/10.1029/2005JD007000, 2007.

McPhaden, M. J.: El Niño and La Niña: causes and global consequences, Encyclopedia of global environmental change, 1, 353–370, 2002.

Merino, M.: Upwelling on the Yucatan Shelf: hydrographic evidence, Journal of Marine Systems, 13, 101–121, https://doi.org/https://doi.org/10.1016/S0924-7963(96)00123-6, 1997.

Mezzina, B., García-Serrano, J., Bladé, I., and Kucharski, F.: Dynamics of the ENSO Teleconnection and NAO Variability in the North Atlantic–European Late Winter, Journal of Climate, 33, 907 – 923, https://doi.org/https://doi.org/10.1175/JCLI-D-19-0192.1, 2020.

Misra, V.: Chapter 6 - Teleconnections, in: Regionalizing Global Climate Variations, edited by Misra, V., pp. 143–174, Elsevier, ISBN 978-0-12-821826-6, https://doi.org/https://doi.org/10.1016/B978-0-12-821826-6.00006-0, 2020.

North, G. R., Bell, T. L., Cahalan, R. F., and Moeng, F. J.: Sampling errors in the estimation of empirical orthogonal functions, Monthly Weather Review, 110, 699–706, https://doi.org/10.1175/1520-0493(1982)110<0699:SEITEO>2.0.CO;2, 1982.

Oey, L.-Y.: Vorticity flux through the Yucatan Channel and Loop Current variability in the Gulf of Mexico, Journal of Geophysical Research: Oceans, 109, https://doi.org/https://doi.org/10.1029/2004JC002400, 2004.

Oey Jr., L.-Y., Ezer, T., and Lee, H.-C.: Loop Current, Rings and Related Circulation in the Gulf of Mexico: A Review of Numerical Models and Future Challenges, pp. 31–56, American Geophysical Union (AGU), ISBN 9781118666166, https://doi.org/https://doi.org/10.1029/161GM04, 2005.

Orihuela-Pinto, B., Santoso, A., England, M. H., and Taschetto, A. S.: Reduced ENSO Variability due to a Collapsed Atlantic Meridional Overturning Circulation, Journal of Climate, 35, 5307 – 5320, https://doi.org/https://doi.org/10.1175/JCLI-D-21-0293.1, 2022.

Pietrafesa, L. J., Bao, S., Gayes, P. T., Carpenter, D. D., and Kowal, J. C.: Variability and Trends of the Florida Current and Implications for the Future of the Gulf Stream, Journal of Coastal Research, 38, 1096–1103, https://doi.org/10.2112/JCOASTRES-D-22A-00006.1, 2022.

Pozo-Vázquez, D., Esteban-Parra, M., Rodrigo, F., and Castro-Díez, Y.: An analysis of the variability of the North Atlantic Oscillation in the time and the frequency domains, International Journal of Climatology, 20, 1675–1692, https://doi.org/https://doi.org/10.1002/1097-0088(20001130)20:14<1675::AID-JOC564>3.0.CO;2-C, 2000.

Reyes-Mendoza, O., Mariño-Tapia, I., Herrera-Silveira, J., Ruiz-Martínez, G., Enriquez, C., and Largier, J. L.: The Effects of Wind on Upwelling off Cabo Catoche, Journal of Coastal Research, 32, 638 – 650, https://doi.org/10.2112/JCOASTRES-D-15-00043.1, 2016.

Ruiz-Castillo, E., Gomez-Valdes, J., Sheinbaum, J., and Rioja-Nieto, R.: Wind-driven coastal upwelling and westward circulation in the Yucatan shelf, Continental Shelf Research, 118, 63–76, https://doi.org/https://doi.org/10.1016/j.csr.2016.02.010, 2016.

Santana-Cisneros, M. L., Ardisson, P.-L., González, A. F., Mariño-Tapia, I., Cahuich-López, M., Ángeles González, L. E., Ordoñez-López, U., and Velázquez-Abunader, I.: Dispersal modeling of octopoda paralarvae in the Gulf of Mexico, Fisheries Oceanography, 30, 726–739, https://doi.org/https://doi.org/10.1111/fog.12555, 2021.

Sheinbaum, J., Candela, J., Badan, A., and Ochoa, J.: Flow structure and transport in the Yucatan Channel, Geophysical Research Letters, 29, 10–1–10–4, https://doi.org/https://doi.org/10.1029/2001GL013990, 2002.

Smith, K. L. and Polvani, L. M.: Modeling evidence for large, ENSO-driven interannual wintertime AMOC variability, Environmental Research Letters, 16, 084 038, https://doi.org/10.1088/1748-9326/ac1375, 2021.

Stocker, T. F. and Schmittner, A.: Influence of CO2 emission rates on the stability of the thermohaline circulation, Nature, 388, 862–865, https://doi.org/10.1038/42224, 1997.

Sturges, W. and Kenyon, K. E.: Mean Flow in the Gulf of Mexico, Journal of Physical Oceanography, 38, 1501 – 1514, https://doi.org/10.1175/2007JPO3802.1, 2008.

Sturges, W. and Leben, R.: Frequency of Ring Separations from the Loop Current in the Gulf of Mexico: A Revised Estimate, Journal of Physical Oceanography, 30, 1814 – 1819, https://doi.org/https://doi.org/10.1175/1520-0485(2000)030<1814:FORSFT>2.0.CO;2, 2000.

Timm, L. E., Isma, L. M., Johnston, M. W., and Bracken-Grissom, H. D.: Comparative Population Genomics and Biophysical Modeling of Shrimp Migration in the Gulf of Mexico Reveals Current-Mediated Connectivity, Frontiers in Marine Science, 7, https://doi.org/10.3389/fmars.2020.00019, 2020.

Trenberth, K. E. and Fasullo, J. T.: Atlantic meridional heat transports computed from balancing Earth's energy locally, Geophysical Research Letters, 44, 1919–1927, https://doi.org/https://doi.org/10.1002/2016GL072475, 2017.

Watanabe, M. and Kimoto, M.: Atmosphere-ocean thermal coupling in the North Atlantic: A positive feedback, Quarterly Journal of the Royal Meteorological Society, 126, 3343–3369, https://doi.org/https://doi.org/10.1002/qj.49712657017, 2000.

Wu, M.-L. C., Schubert, S. D., Suarez, M. J., Pegion, P. J., and Waliser, D. E.: Seasonality and Meridional Propagation of the MJO, Journal of Climate, 19, 1901 – 1921, https://doi.org/10.1175/JCLI3680.1, 2006.

Yang, Y., Weisberg, R. H., Liu, Y., and Liang, X. S.: Instabilities and Multiscale Interactions Underlying the Loop Current Eddy Shedding in the Gulf of Mexico, Journal of Physical Oceanography, 50, 1289 – 1317, https://doi.org/10.1175/JPO-D-19-0202.1, 2020.

Zavala-Hidalgo, J., Morey, S. L., and O'Brien, J. J.: Cyclonic Eddies Northeast of the Campeche Bank from Altimetry Data, Journal of Physical Oceanography, 33, 623 – 629, https://doi.org/10.1175/1520-0485(2003)033<0623:CENOTC>2.0.CO;2, 2003.

Zavala-Hidalgo, J., Gallegos-García, A., Martínez-López, B., Morey, S. L., and O'Brien, J. J.: Seasonal upwelling on the Western and Southern Shelves of the Gulf of Mexico, Ocean Dynamics, 56, 333–338, https://doi.org/10.1007/s10236-006-0072-3, 2006.

Zavala-Hidalgo, J., Romero-Centeno, R., Mateos-Jasso, A., Morey, S. L., and Martínez-López, B.: The response of the Gulf of Mexico to wind and heat flux forcing: What has been learned in recent years?, Atmósfera, 27, 317–334, https://doi.org/https://doi.org/10.1016/S0187-6236(14)71119-1, 2014.